Application Note

Invasive aspergillosis-on-chip

Quantitative Analysis of human lung infection treatments caused by *Aspergillus fumigatus*

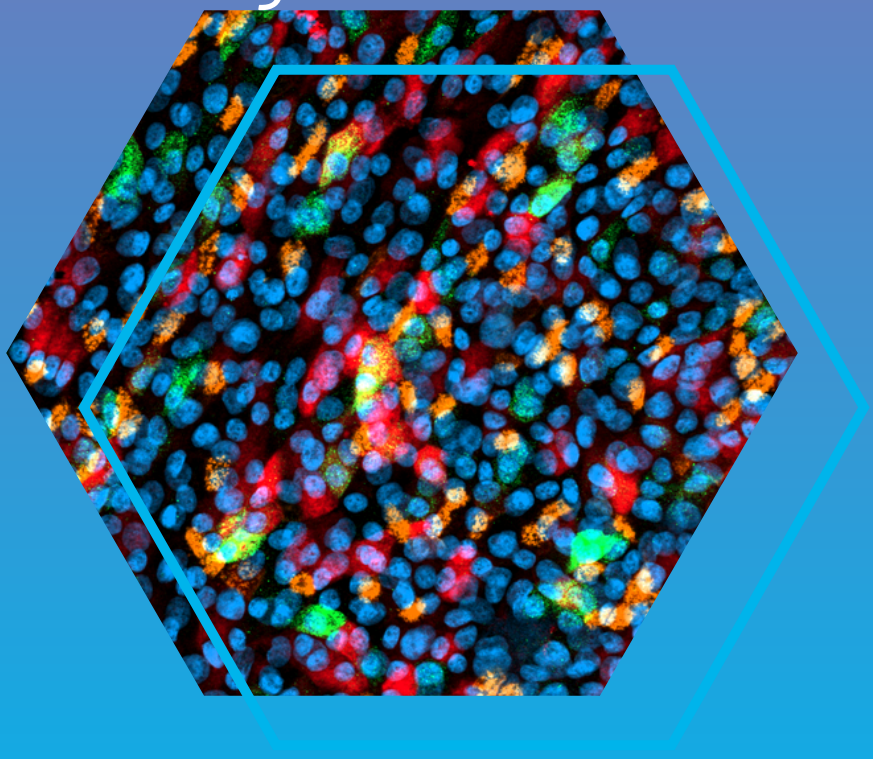

Author:
Dr. Mai Hoang

Release data:
05/06//2024

Abstract

Lung infections have emerged as a critical concern in recent times, driven by the increasing number of drug-resistant microorganisms. The complexity of lung infections demands models that can mimic the intricate interplay between pathogens and residential host cells. The current application models Aspergillus fumigatus (*A. fumigatus*) fungal invasion in the human lung alveolus. In this invasive aspergillosis on chip (IAC) model, *A. fumigatus* conidia are challenged by human primary monocyte-derived macrophages. Fungal hyphae growth parameters (e.g., length, branching level) and number of invasive hyphae are altered in the presence of macrophages. Antifungal drugs such as Caspofungin, when administered at clinically relevant concentrations also induced known morphological changes in *A. fumigatus* hyphae.
Thus, this immunocompetent model offers a complex representation of lung tissue structure and function, offering a reliable platform for antifungal drug development and improving our understanding of fungal pathogenicity.

Highlights

- The IAC model provides a physiologically relevant platform for studying the pathogenicity of *A. fumigatus* fungal infection.
- This model mimics invasive growth of *A. fumigatus* hyphae from the lung alveolar epithelium to the surrounding vasculature.
- The growth parameters of *A. fumigatus* hyphae are altered in the presence of macrophages or as a result of antifungal drug administration.
- Dynamic42 lung-on-chip model serves as a focal point for studying lung infections like *A. fumigatus*, highlighting their advantages in accurately representing lung tissue structure and function compared to traditional culture systems.

Introduction

Invasive pulmonary aspergillosis (IPA) poses a critical risk for immunocompromised individuals, such as those receiving hematopoietic stem cells or organ transplants. If left untreated, IPA is almost always fatal (4). In healthy people, alveolar macrophages defend the lungs by recognizing and engulfing pathogens like *A. fumigatus* conidia. Without proper immune defense, conidia can develop into hyphae, damaging lung tissue and invading blood vessels. In vitro IPA studies often use static confrontation assays, while advanced models with air-liquid interfaces study epithelial infections but overlook endothelial cells. Mouse models exist, but physiological differences limit their effectiveness. Leveraging a human alveolus model, termed the invasive aspergillosis-on-chip (IAC), we replicate human lung features, allowing detailed analysis of hyphae formation and antifungal drug testing. This application note presents a detailed protocol for the implementation of the alveolus on chip model to study invasive aspergillosis. The methodology and results described herein is adapted from the study conducted by Hoang et al., published in Biomaterials (2022), titled "Invasive aspergillosis-on-chip: A quantitative treatment study of human *Aspergillus fumigatus* infection"

Materials and Methods

The materials and methods outlined in this application note closely follow those outlined in Hoang et al. 2022 (9). Any modifications or adaptations made to the protocol are clearly specified.

Peristaltic pump

(can be purchased in line with the DynamicOrgan System)

DynamicOrgan Developers Kit

Including:
/ Biochips (BC002)
/ 2-Stop Tubing
/ Connectors (Adapter)
/ Reservoirs

Cells and fungal strains (9)

NCI-H441 cells
Human umbilical vein endothelial cells (HUVECs)
Monocyte-derived macrophages
Aspergillus fumigatus A1160 (wildtype)

Media and reagents (9)

Endothelial cell growth medium + supplements
RPMI 1640
Aspergillus minimal medium

Results

1. The alveolus on chip model for IPA

Briefly, in a standard Dynamic42 biochip containing a polyethylene-terephthalate (PET) membrane with randomly distributed pores (median density: 1 × 105 cm2) of 8 µm in diameter, HUVEC and NCI-H441 cells were seeded consecutively on opposite sides of the membrane, yielding the endothelial and epithelial side, respectively. After 7 days, human macrophages derived from monocytes obtained by PBMC isolation were seeded onto the NCI-H441 cells (detailed in 7). Up to this point, the biochips were cultured statically. The next day, perfusion of the endothelial side was commenced using a peristaltic pump. The suitable media were pumped from a reservoir through the respective chamber in a closed-loop system. Medium in the reservoirs was changed daily. On day 13, the ALI was initiated by the removal of media from the epithelial side. All cells in the chip are nurtured by the perfused media on the endothelial side. Biochips were used for experiments after total cultivation of 14 days. Figure 1 shows the characterization of the alveolus model that can be used for the subsequent infection with *A. fumigatus* conidia.

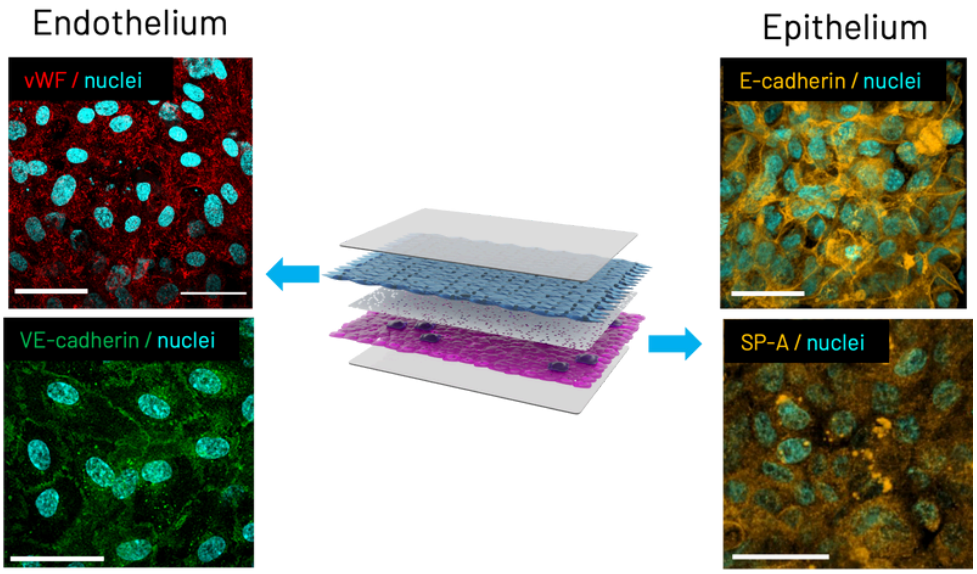

Figure 1: Immunofluorescence staining of: left panel: endothelial cell layer by von Willebrand factor (vWF, red) and VE-cadherin (green), right panel: epithelial cell layer by E-cadherin (orange) and surfactant protein A (SP-A, orange), mid-panel: 3D view of endothelial (blue) and epithelial (magenta) cell layer including marcophages (purple). Scale bars = 50µm. Figure adapted from Fig.2 in Ref. 9.

2. The lung-on-chip model mimics the stages of invasive aspergillosis during fungal infection

In our alveolus model, we simulated invasive pulmonary aspergillosis (IPA) by temporarily infecting the epithelial cell layer with resting fluorescein isothiocyanate (FITC)-labeled *A. fumigatus* conidia, which are approximately 2 µm in size. The infection was initiated by introducing a suspension containing a concentration of 1 × 103 conidia per square micrometer, administered under static conditions. After overnight incubation with perfusion of the endothelial cell layer, hyphal growth was evident, predominantly on the epithelial side, with minimal damage to the epithelial layer observed (Fig. 2A). Furthermore, invasive fungal growth into the endothelial side of the alveolus model was detected, leading to localized destruction of the endothelial layer (Fig. 2A, C). On average, 32 conidia per image were detected on the epithelial side, while only two conidia per image were found on the endothelial side (Fig.2B).

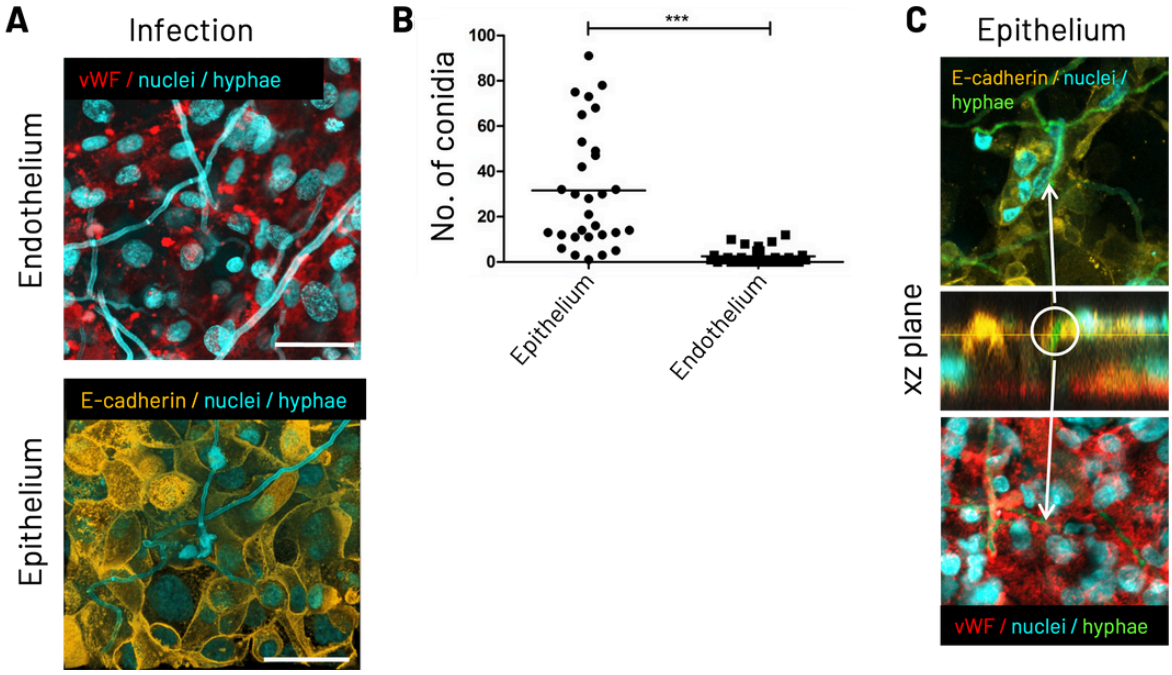

Figure 2: Fungal growth in the IAC model. Epithelial cells stained by E-cadherin (orange) and endothelial cells stained by von Willebrand factor (vWF, red) in A) not infected controls and B) *A. fumigatus* infected IAC models. Hyphae stained by Calcofluor white (CFW) in blue (long filaments). Nuclei stained by Hoechst 33258 in blue (elliptic circles). Scale bars = 50µm. C) Conidial counts were high on the epithelium, but usually no conidia were found in the endothelium. Mean is indicated by a line. Unpaired two-tailed t-test. *** p<0.001. D) Invasive hyphal growth from the epithelium (E-cadherin, orange, top) to the endothelium (vWF, red, bottom) shown by constitutively eGFP-positive *A. fumigatus* mutant (green). Hyphae growing vertically through both layers (white circle, middle) with points of penetration indicated by white arrows. Figure adapted from Fig.2 in Ref. 9.

3. Macrophages altered fungal invasion behavior and induced inflammatory responses in the IAC model

When cultivated overnight in the presence of macrophages and under perfusion, *A. fumigatus* horizontal hyphal growth was restricted (averaging 329 ± 319 µm) (Fig.3A). In contrast, the mean branching levels (2 ± 1), and germination rate showed only minor changes (Fig.3 B-C). There was notable diversity among the three macrophage donors regarding each hyphal parameter, which obscured potential significant differences between conditions when averaging across all three experiments. As a result, discernible alterations were chiefly observed when comparing conditions within each donor's dataset, while the general trend remained consistent across different donors. Furthermore, macrophages exerted influence over the orientation of hyphal growth. In the absence of macrophages,
A. fumigatus hyphae, notably elongated, spread across the epithelial side of the IAC model (Fig. 3E, lateral (XY) view), occasionally breaching the membrane pores to access the endothelial side (Fig. 3E, axial (XZ) view). Although a reduced number of hyphae were observed in the presence of macrophages, approximately 37 ± 7% of these displayed invasiveness (Fig. 3D), marking a threefold increase compared to the absence of macrophages (averaging 12 ± 5%, $p < 0.01$, Fig. 3D).

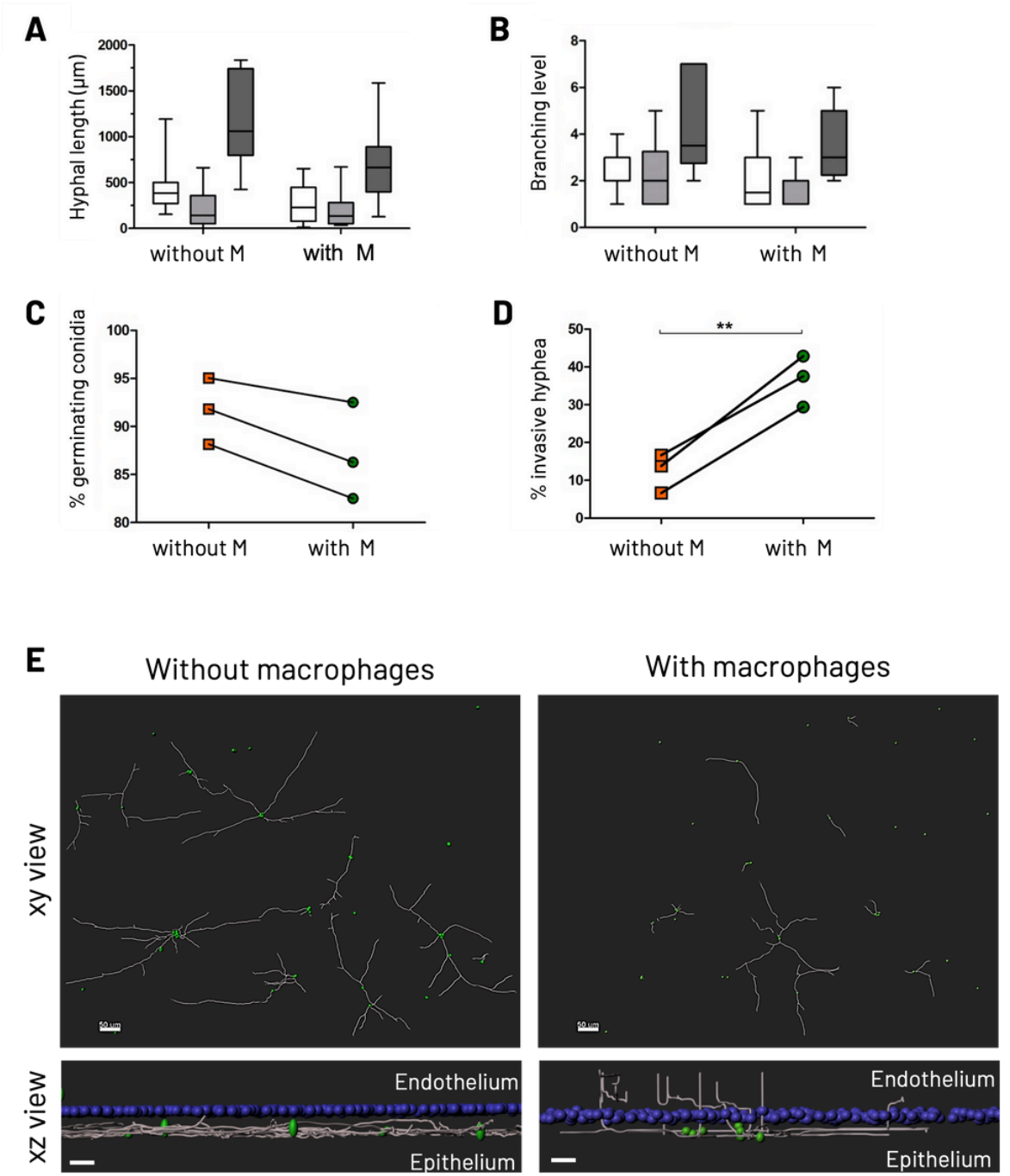

Figure 3: Partial inhibition of *A. fumigatus* growth by human macrophages. Bioimage analysis-based quantification of A) hyphal length, B) branching level. Box and whiskers plot of three independent experiments (shades of grey, 6–27 hyphae analyzed per experiment) with three different macrophage donors. Boxes represent quartiles around median (line). Whiskers indicate minima and maxima. C) Percentage of germinated conidia in IAC models with and without macrophages from three independent experiments with three different macrophage donors. D) Percentage of invasive hyphae in IAC models with and without macrophages from three independent experiments with three different macrophage donors. Unpaired two-tailed t-test, ** $p<0.01$. E) Reconstructions of *A. fumigatus* hyphae from IAC models with and without macrophages presented as top view (xy view) and as lateral view (xz view) of the epithelial side show length and direction of fungal growth. Grey lines represent hyphae, green spots represent conidia, blue spots in xz view represent membrane pores. Scale bars = 50µm. Figure adapted from Fig.3 and 4 in Ref. 9.
M: Macrophages

Further characterization of the macrophage response to *A. fumigatus* in the IAC model involved studying cytokine release in the alveolus 14 h post-infection, both with and without macrophages (Fig.4). On the epithelial side, the amount of pro-inflammatory cytokines IL-1β (Fig.4A) and IL-6 (Fig.4B) was increased in the presence of macrophages (average IL-1β: 7.0 ± 5.6 pg/ml and IL-6: 479 ± 372 pg/ml, compared to controls without macrophages IL-1β: 0.8 ± 0.6 pg/ml and IL-6: 195 ± 128 pg/ml). Because of significant variability between individuals, the observed distinctions did not achieve statistical significance. Intriguingly, our investigation revealed no indications supporting heightened invasiveness correlating with elevated cytokine levels, indicating that increased permeability might not be the underlying factor driving heightened invasiveness.

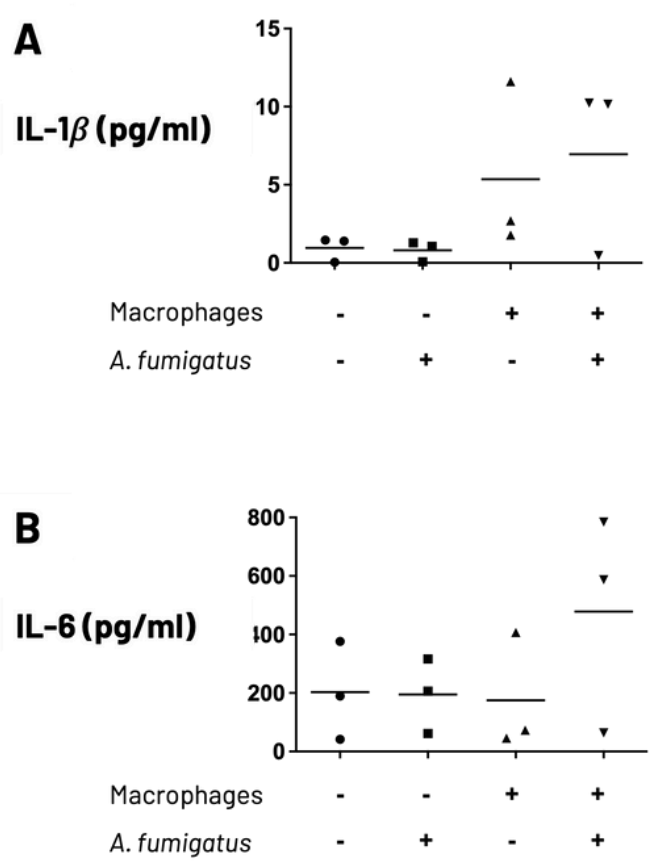

Figure 4: Cytokine release in IAC models upon *A. fumigatus* infection. Pro-inflammatory cytokines IL-1β (A), and IL-6 (B) were detected separately on the epithelial side of IAC models with and without macrophages in presence or absence of *A. fumigatus*. Each data point presents results obtained by multiplex-assays from three independent experiments (n=3) with three different macrophage donors. Lines represent means. One-way ANOVA with Bonferroni post-test. Figure adapted from Fig.5 in Ref. 9.

4. Caspofungin elicits characteristic morphological transformations in fungal hyphae

Caspofungin only stalled hyphal growth (Fig.5). This effect was most notable at 0.5 µg/ml (mean hyphal length 222 ± 156 µm) compared to untreated controls (mean hyphal length 1775 ± 1462 µm, $p < 0.001$), reversing at 5 µg/ml (mean hyphal length 741 ± 659 µm). Consistent with previous studies (5, 6), caspofungin led to colony formation and altered hyphal morphology, showing shorter, thicker hyphae (Fig.5A,B). Caspofungin increased branching, notably at 5 µg/ml (mean branching level 6 ± 4, mean number of branches 23 ± 31) (Fig. 5C). While branch numbers per hypha and branching levels didn't differ significantly, caspofungin-treated samples showed denser branching (Fig.5D,E)

Invasive growth occurred alongside horizontal growth, with control infections exhibiting the highest percentages of invasive hyphae, averaging 53 ± 50% (Fig.6A). Although caspofungin decreased invasive hyphae, it didn't entirely prevent invasion (mean percentages: 47 ± 12% at 0.05 µg/ml, 10 ± 10% at 0.5 µg/ml, and 18 ± 17% at 5 µg/ml caspofungin) (Fig.6B).

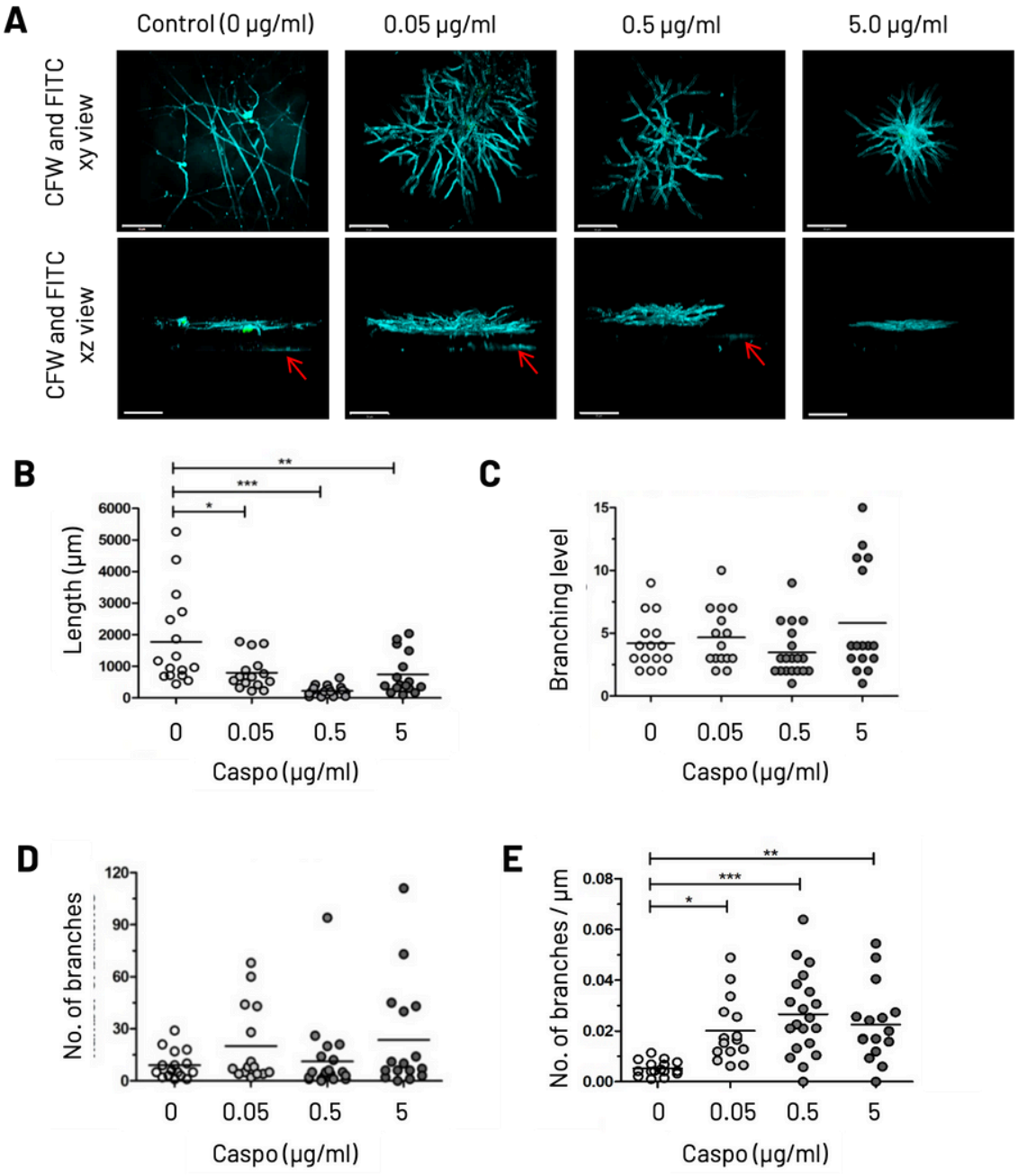

Figure 5: IAC model as a platform for drug testing. A) Application of caspofungin at increasing concentrations (0.05, 0.5 and 5µg/ml) yielded known morphological changes in terms of filament length and clustering (top panel: xy plane, bottom panel: xz plane). Red arrows indicate invasive hyphae grown from the epithelial to the endotehlial layer. Hyphae stained by CFW. Scale bars = 50µm. B-E) Bioimage analysis of hyphae from untreated and caspofungin-treated IAC models revealed significant differences in filament length, but neither in the number of branches, nor branching level. Dot plots show results from three independent experiments with 5–8 hyphae analyzed per condition and experiment, with the line indicating the mean. * $p<0.05$, ** $p<0.01$, *** $p<0.001$ (one-way ANOVA with Bonferroni post-test). Figure adapted from Fig.6 in Ref. 9.
CFW: Calcofluor White

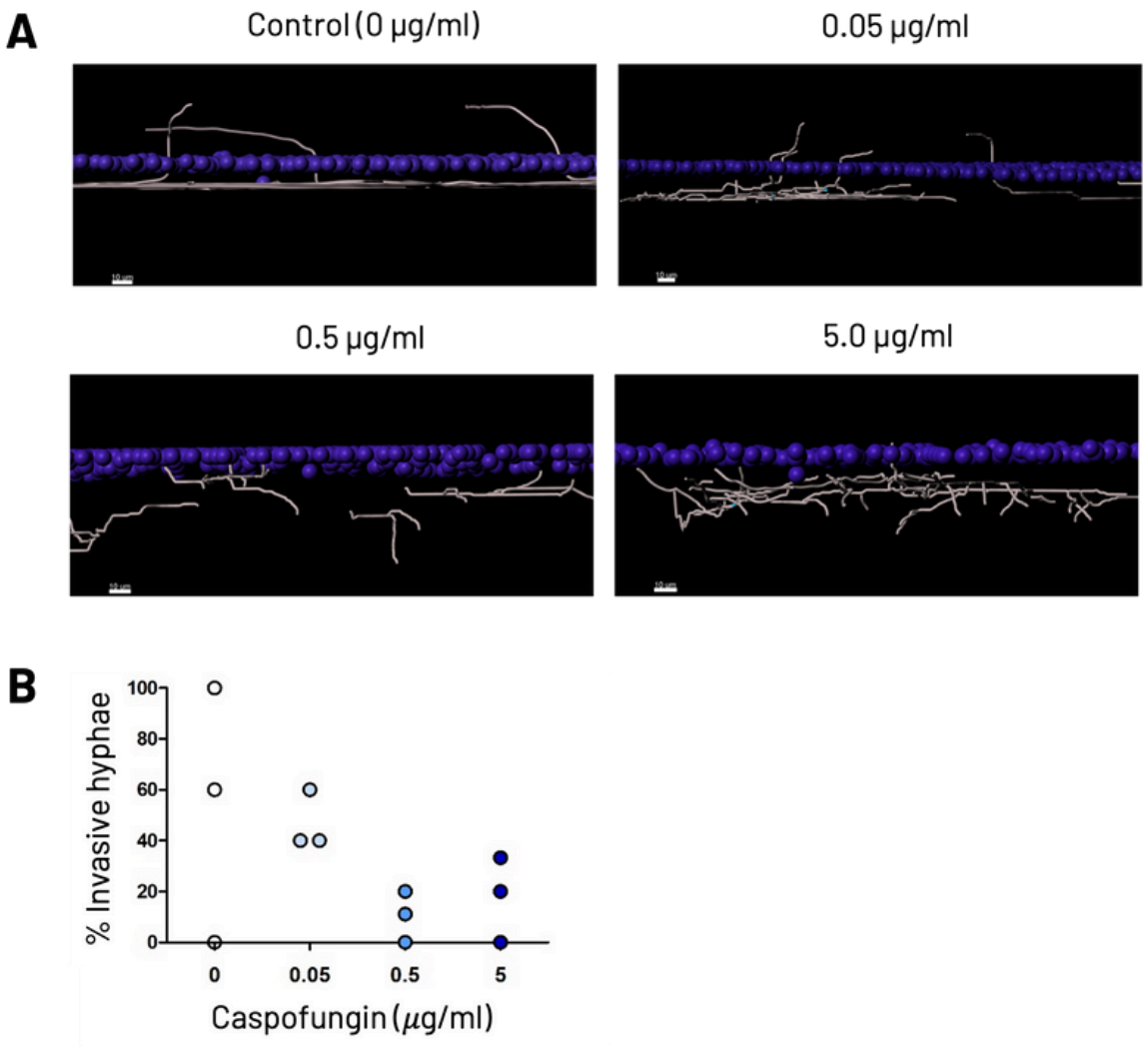

Figure 6: Modulation of invasive hyphal growth at therapeutic levels of caspofungin. A) Reconstructions of *A. fumigatus* hyphae from IAC models treated without (control, 0 µg/ml) or with increasing concentrations of caspofungin as lateral view (xz view) showing invasive fungal growth. Grey lines represent hyphae, blue spots represent membrane pores. Scale bars = 10µm. B) Percentage of invasive hyphae in untreated models or caspofungin-treated models from three independent experiments. Figure adapted from Fig.7 in Ref. 9.

Conclusion

The alveolus-on-a-chip previously demonstrated the ability to create a physiologically relevant environment, exhibiting strong barrier function and effective immune responses against pathogens (7). Here, it is demonstrated that the IAC model effectively replicates key stages of invasive aspergillosis, making it a valuable tool for studying fungal infections. FITC-labeled *A. fumigatus* conidia successfully reached the alveolar region, and overnight incubation led to significant hyphal growth on the epithelial surface, and consequently invading vascular side. Subsequently, by taking advantage of this three-dimensional nature of the IAC model and leveraging advanced imaging and image analysis techniques, we were able to obtain quantitative data on fungal morphology including hyphal length, branching, germination, and invasion behavior. This strongly suggested that our IAC model provided a more reliable means of quantifying the growth and invasion behavior of individual hyphae compared to conventional two-dimensional studies (1, 2, 3).

Additionally, the involvement of primary human macrophages in our investigation played a key role in clarifying the interactions between macrophages and *A. fumigatus* conidia. Variability among macrophage donors obscured significant differences, but trends were consistent within individual donors. Notably, macrophages increased the invasiveness of hyphae, with a higher percentage of hyphae penetrating the membrane compared to when macrophages were absent. Additionally, the presence of macrophages increased the release of pro-inflammatory cytokines such as IL-1β and IL-6 on the epithelial side, aiding in the recruitment of immune cells.

Furthermore, we also showed that administering of clinically relevant concentration of antifungal drugs, such as Caspofungin, induced morphological changes in fungal hyphae. Specifically, Caspofungin increased the branching density of hyphae, reduce the number of invasive hyphae, but did not completely prevent hyphal invasion into the endothelial side.

In conclusion, this application strongly suggests that IAC model could offer a highly physiologically relevant platform for investigating fungal pathogenicity and developing novel antifungal therapeutics, as demonstrated by Hoang et al. 2022 (9).

Key takeaways

- The IAC model effectively replicates invasive aspergillosis stages, offering insights into fungal infections' progression.
- Advanced imaging and analysis techniques in the IAC model provide detailed quantitative data, surpassing conventional 2D studies in understanding fungal pathogenesis.
- Macrophages alter *A. fumigatus* growth patterns, limiting hyphal growth but increasing invasiveness and pro-inflammatory cytokine release.
- Caspofungin treatment stalls hyphal growth and increases branching density, yet fails to fully prevent hyphal invasion.

References

1. D.J. Barry, G.A. Williams, Microscopic characterisation of filamentous microbes: towards fully automated morphological quantification through image analysis, J Microsc, 244 (1)(2011), pp. 1-20
2. G. Sanchez-Orellana, S. Casas-Flores, B. Gutierrez-Medina, Automated, continuous video microscopy tracking of hyphal growth, Fungal Genet. Biol., 123 (2019), pp. 25-32
3. G. Vidal-Diez de Ulzurrun, et al., Fungal feature tracker (FFT): a tool for quantitatively characterizing the morphology and growth of filamentous fungi, PLoS Comput. Biol., 15 (10)(2019), Article e1007428
4. J.P. Latge, Aspergillus fumigatus and aspergillosis, Clin. Microbiol. Rev., 12 (2)(1999), pp. 310-350
5. Espinel-Ingroff, et al., Wild-type MIC distributions and epidemiological cutoff values for caspofungin and Aspergillus spp. for the CLSI broth microdilution method (M38-A2 document). Antimicrob. Agents Chemother., 55 (6)(2011), pp. 2855-2859
6. EUCAST Technical Note on the method for the determination of broth dilution minimum inhibitory concentrations of antifungal agents for conidia-forming moulds., Clinical microbiology and infection: the official publication of the European Society of Clinical Microbiology and Infectious Diseases, 14 (10)(2008), pp. 982-984
7. S. Deinhardt-Emmer, et al., Co-infection with Staphylococcus aureus after primary influenza virus infection leads to damage of the endothelium in a human alveolus-on-a-chip model, Biofabrication, 12 (2)(2020), p. 25012
8. S. Hutner, et al., Some approaches to the study of the role of metals in the metabolism of microorganisms, Proc. Am. Phil. Soc., 94 (1950), pp. 152-170
9. T.N.M Hoang, et al., Invasive aspergillosis-on-chip: A quantitative treatment study of human Aspergillus fumigatus infection, Biomaterials, 283 (2022)

DYNAMIC42

Get in touch

Email
info@dynamic42.com

Web
dynamic42.com

Join us

Head Office
+49 (0) 3641 508101

Dynamic42 GmbH
Winzerlaer Straße 2
07745 Jena
Germany